

Reducing off-target expression of mRNA therapeutics and vaccines in the liver with microRNA binding sites

Brian J. Parrett,¹ Satoko Yamaoka,² and Michael A. Barry^{2,3,4}

¹Virology and Gene Therapy (VGT) Graduate Program, Mayo Clinic, Rochester, MN 55902, USA; ²Department of Medicine, Division of Infectious Diseases, Mayo Clinic, Rochester, MN 55902, USA; ³Department of Immunology, Mayo Clinic, Rochester, MN 55902, USA; ⁴Department of Molecular Medicine, Mayo Clinic, Rochester, MN 55902, USA

Lipid nanoparticles (LNPs) are often liver tropic, presenting challenges for LNP-delivered mRNA therapeutics intended for other tissues, as off-target expression in the liver may increase side effects and modulate immune responses. To avoid off-target expression in the liver, miR-122 binding sites have been used by others in viral and non-viral therapeutics. Here, we use a luciferase reporter system to compare different copy numbers and insertion locations of miR-122 binding sequences to restrict liver expression. We inserted one to five miR-122 binding sites into the 5' or 3' untranslated regions (UTRs) of luciferase mRNAs and tested them in LNPs *in vitro* and *in vivo* via systemic intravenous and local intramuscular injections in mice. Our results showed no significant differences in de-targeting efficacy between mRNAs harboring one or multiple miR-122 binding sites or between those with 5' or 3' UTR placements. To test the impact of miR-122 binding sites on antibody response to a mRNA vaccine, Ebola virus matrix protein VP40 mRNAs were modified with or without miR-122 binding sites and injected in mice intramuscularly. This work reinforces the utility of miR-122 binding sites while providing a comparison of these sites to aid the future development of LNP-mRNA therapies for non-hepatic tissues.

INTRODUCTION

Lipid nanoparticles (LNPs) are potent non-viral vectors for the delivery of RNA therapeutics.^{1,2} Billions of doses of LNPs carrying SARS-CoV-2 Spike mRNA have been administered to humans by the intramuscular (IM) route.^{3,4} In most cases these LNPs are formulated with four components, including an ionizable lipid, a helper lipid, a PEGylated lipid, and cholesterol. *In vivo*, LNPs enter cells by forming a complex with circulating apolipoproteins that facilitate binding and entry via the low-density lipoprotein receptor (LDLR).^{5–7} Although LDLR is ubiquitous in all mammalian cells and LNPs can transfect many cell types, the primary organ that is targeted by LNPs after an intravenous (IV) injection is the liver due to its high expression of LDLR and easy access to hepatocytes through fenestrations in the liver vasculature. While this high liver transfection may be ideal for liver-directed therapy, this is problematic if one is attempting to target therapies to other tissues by the IV route.

Off-target transfection of the liver can also be a problem when injecting LNP-mRNA by non-IV routes, since LNPs are documented to leak into the bloodstream and reach the liver regardless of their original site of injection. For example, as much as 21.5% of the LNPs of COVID-19 mRNA-LNP vaccines injected via the IM route were found in the liver in preclinical studies.^{8,9} These mRNA vaccines have been shown to be safe; however, the extent of LNP leakage in humans is unclear.

RNA interference (RNAi) plays a critical role in regulating the expression of cellular mRNAs. After processing, microRNAs (miRNAs) are loaded into the RNA-induced silencing complex, which then targets mRNAs containing complementary binding sequences to the miRNA and facilitates translational repression and degradation.¹⁰ Addition of miRNA target sites to viral vectors has proven effective by others in controlling tissue-specific expression and organ de-targeting in various applications such as molecular therapy or oncolytic viral vectors.^{11–18} miR-122 is the most abundant miRNA in the liver, making miR-122 an ideal tool to de-target expression in the liver by inserting miR-122 binding sites into mRNAs. Modification of LNP-mRNA therapeutics with miR-122 binding sites have also been used previously by others as an effective way to prevent the expression of mRNAs in healthy liver cells.^{19–21}

To complement this prior art, we used a luciferase reporter system to conduct a detailed characterization of miR-122 binding site insertion in LNP-mRNA to evaluate how the number of copies and insertion locations impact its potency for liver de-targeting. We hypothesized that expression levels in the liver would vary depending on the number of copies or the location of insertion of miR-122 binding sites. To examine this hypothesis, luciferase mRNAs were modified by inserting 1–5 miR-122 binding sites into the 5' or 3' untranslated regions (UTRs). Modified and unmodified mRNAs were encapsulated into

Received 18 May 2024; accepted 17 December 2024;
<https://doi.org/10.1016/j.omtm.2024.101402>.

Correspondence: Michael A. Barry, Department of Medicine, Division of Infectious Diseases, Mayo Clinic, 200 First Street SW, Rochester, MN 55902, USA.
E-mail: mab@mayo.edu



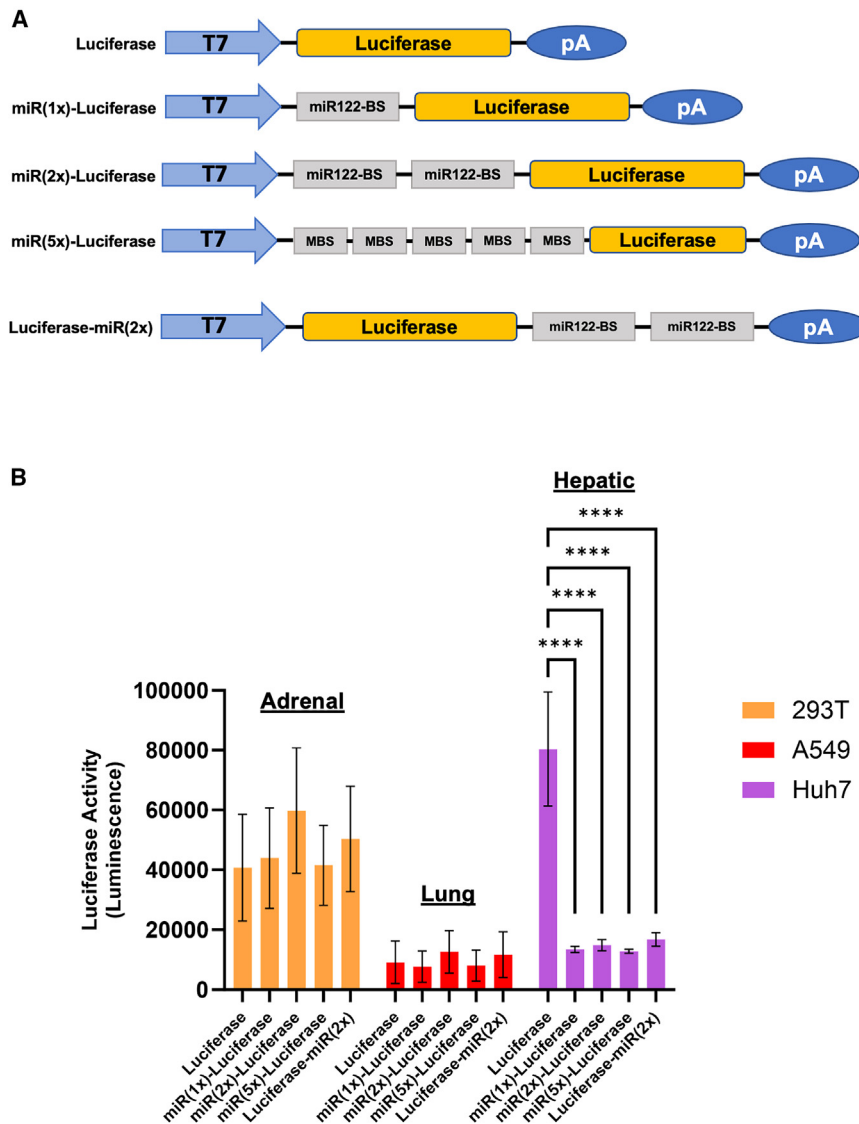


Figure 1. Comparison of luciferase reporter expression between mRNA with and without miR-122 binding site modifications

(A) Illustration of T7 luciferase DNA plasmid constructs for producing miR-122 binding site-modified and unmodified luciferase mRNA via IVT. MBS, miR-122 binding site; pA, poly(A) tract; T7, T7 promoter. (B) Comparison by one-way ANOVA of unmodified and miR-122-modified luciferase mRNA expression in hepatic (Huh7), adrenal (293T), and lung (A549) cell lines. There were significant reductions in luciferase activity of all modified mRNAs in hepatic cells ($****p \leq 0.0001$), but no significant differences in expression were observed in non-hepatic cells. Data represents mean \pm SD.

mRNA sequence (Figure 1A). mRNAs were synthesized with T7 polymerase by *in vitro* transcription (IVT), purified, then loaded into LNPs consisting of 1,2-distearoyl-sn-glycero-3-phosphocholine (DSPC), cholesterol, dilinoleylmethyl-4-dimethylaminobutyrate (D-Lin-MC3-DMA), 1,2-dimyristoyl-rac-glycero-3-methoxypolyethylene glycol-2000 (DMG-PEG2000) at a molar ratio of 10:48:40:2, respectively, a formulation shown by others to effectively deliver nucleic acids.^{1,22} A microfluidic system was used to assemble LNP-mRNA, and mRNA packaging efficiency, size, and particle concentrations were measured.

When human Huh7 hepatic cells were transfected with LNP-mRNA, miRNA-modified mRNAs mediated approximately 80% (5.6-fold) lower luciferase expression than the unmodified luciferase mRNA (Figure 1B). In contrast, when the same LNP-mRNAs were used to transfect non-hepatic human 293T adrenal cells or human A549 lung cells, no significant difference in luciferase expression was

observed between the unmodified and miRNA binding site modified mRNAs (Figure 1B). These data validated the functionality of our constructs and show that inclusion of the miR-122 binding site retained normal reporter expression in non-hepatic cells but limited expression in hepatic cells. There was no statistically significant difference in the miR-122 binding site-mediated reduction of reporter expression in Huh7 hepatic cells between mRNAs with one or multiple miR-122 binding sites, which was also true of mRNAs with the binding sites in the 5' or 3' UTR.

RESULTS

miR-122 binding sites limit luciferase expression in hepatic cells but preserve expression in non-hepatic cells

To evaluate the effect of miR-122 binding sites on the expression of mRNAs, a luciferase reporter system was used. The firefly luciferase cDNA was cloned into a plasmid containing an upstream T7 promoter and downstream polyadenosine tract. One to five copies of miR-122 binding sites were inserted into the 5' or 3' UTR of the luciferase

observed between the unmodified and miRNA binding site modified mRNAs (Figure 1B). These data validated the functionality of our constructs and show that inclusion of the miR-122 binding site retained normal reporter expression in non-hepatic cells but limited expression in hepatic cells. There was no statistically significant difference in the miR-122 binding site-mediated reduction of reporter expression in Huh7 hepatic cells between mRNAs with one or multiple miR-122 binding sites, which was also true of mRNAs with the binding sites in the 5' or 3' UTR.

LNP-mRNA expression in the liver is reduced by the inclusion of miR-122 binding sites after IV injection

To test the de-targeting efficacy of these miR-122 modifications *in vivo*, LNPs carrying luciferase, miR-122(1 \times)-luciferase, miR-122(2 \times)-luciferase, miR-122(5 \times)-luciferase, or luciferase-miR-122(2 \times) mRNAs (Figure 1A) were administered by a single IV injection via

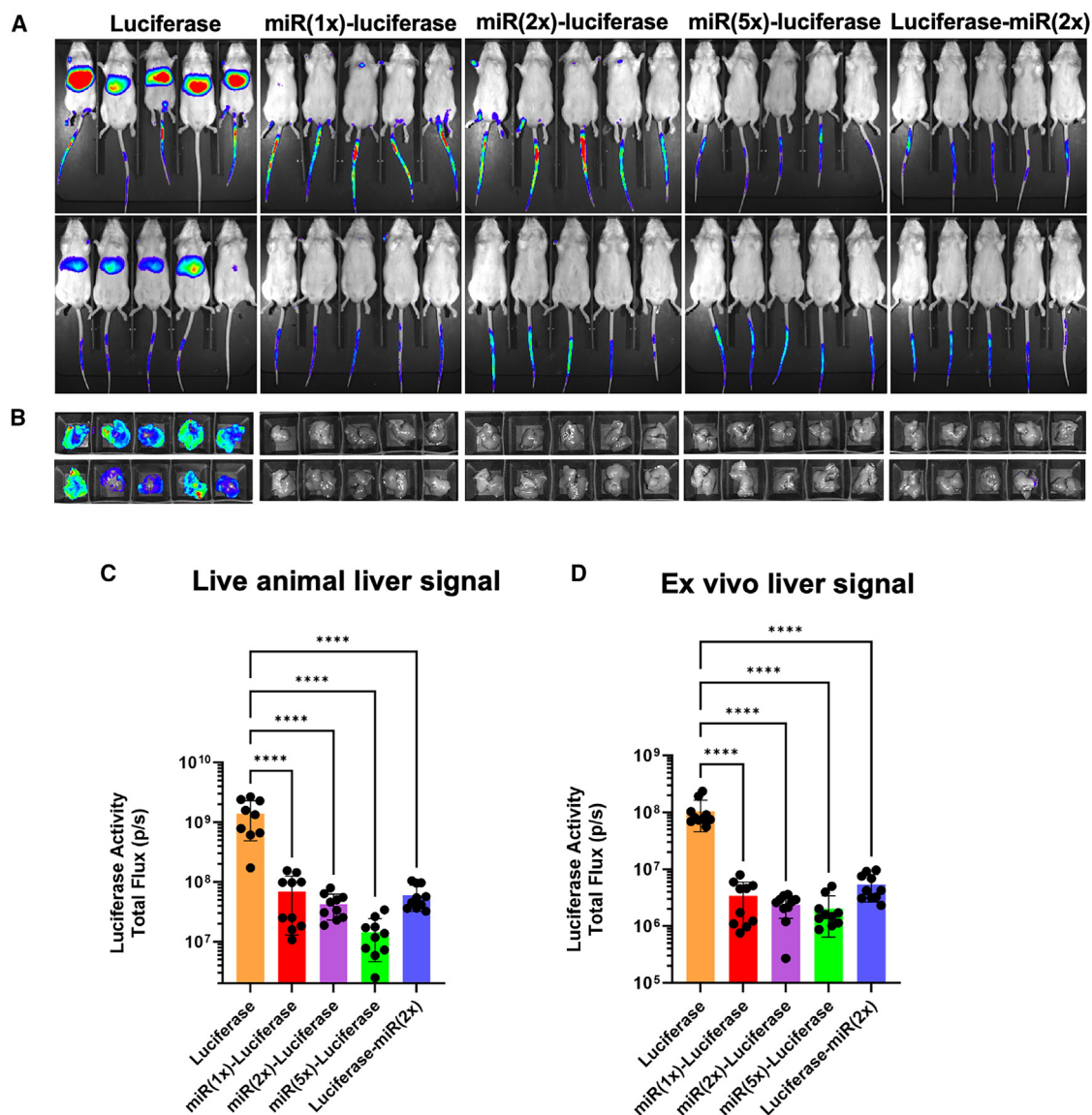


Figure 2. LNP liver de-targeting of miR-122 binding site-modified mRNA after systemic delivery in mice

(A) Groups of five mice were injected with 14 μ g modified or unmodified LNP-mRNA via the tail vein. (B) Luciferase activity was measured in live animals 18 h post-injection, followed by imaging of livers *ex vivo*. (A and B, top and bottom) Two different experiments. (C and D) miR-122 mRNA modification yields significant reductions in liver luciferase activity in both (C) the live animal and (D) the *ex vivo* liver, regardless of the quantity or location of the binding site. Comparison by one-way ANOVA; **** $p \leq 0.0001$. p/s, photons/s. Data represents mean \pm SD.

the tail vein in mice. The mice were then imaged to quantify luciferase activity in the liver 18 h after injection. Live animal imaging and *ex vivo* imaging of organs demonstrated that IV injection of LNPs carrying unmodified luciferase mRNA produced strong luciferase expression in the liver (Figures 2A and 2B). In contrast, LNPs carrying miR-122-modified-luciferase mRNA payloads had 94% to 99% (50-fold average) reductions in luciferase activity in the liver compared to the unmodified mRNA (Figures 2C and 2D). These data demonstrate that inclusion of miR-122 binding sites in the LNP-delivered mRNA restricts expression in the liver even when

delivered systemically via an IV injection. Importantly, these de-targeting effects were not due to a fundamental deficiency in the expression of miRNA binding site modified mRNAs, since injection of the LNP-mRNA with the miRNA binding sequences into the muscles of mice did not show a decrease in luciferase activity (Figure 3). Expression *in vitro* also did not indicate defects in luciferase expression in non-hepatic cells caused by miR-122 binding sequence inclusion (Figure 1B). Consistent with our *in vitro* findings, no statistically significant difference in luciferase activity was seen in the liver regardless of the quantity of copies or

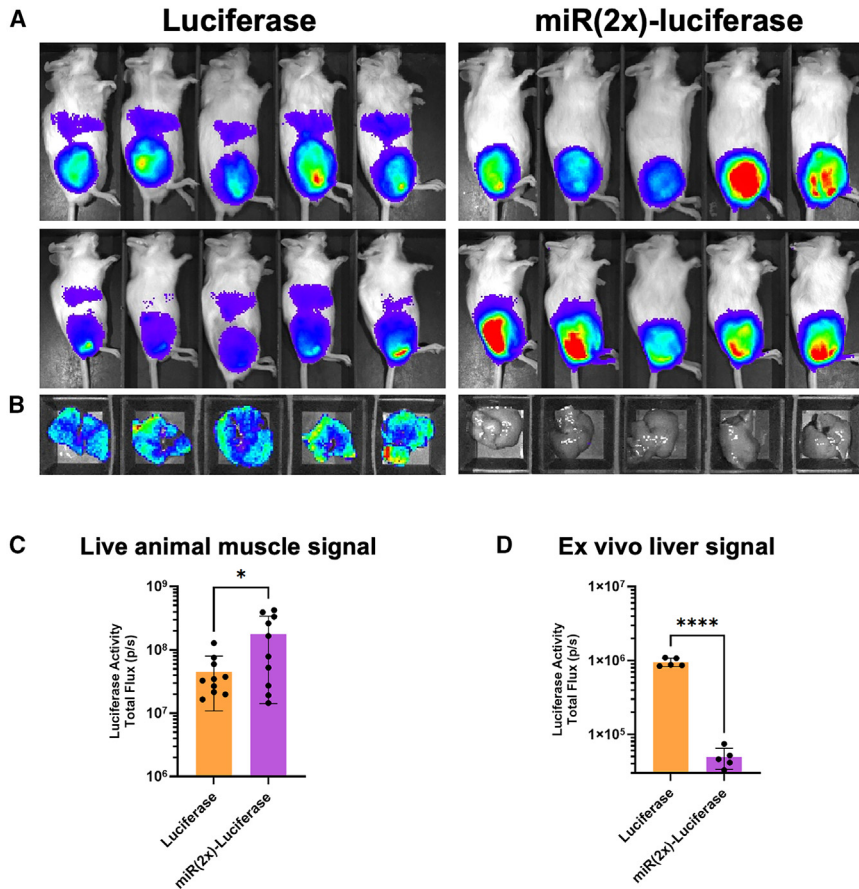


Figure 3. LNP liver de-targeting of miR-122 binding site-modified mRNA delivered via intramuscular injection

(A) Groups of five mice were injected with LNP-mRNA with or without miR-122 binding site sequence in the right quadriceps. Luciferase activity in live animals was measured 18 h post-injection. Top and bottom: two different experiments. (B) Livers were excised and imaged *ex vivo*. (C) Comparison of luciferase signal in the hind flank, unpaired t test ($*p = 0.0221$). (D) Comparison of luciferase signal in the liver. Statistics by unpaired t test ($****p \leq 0.0001$). p/s, photons/s. Data represents mean \pm SD.

luciferase mRNA had slightly higher expression in their muscles but had 95% (19.3-fold) reductions in liver luciferase expression (Figures 3B–3D).

LNP-mRNA vaccine encoding EBOV VP40 with miR-122 binding sites

De-targeting of an mRNA-LNP vaccine and preventing antigen expression in the liver may reduce the risks of side effects. It might also enhance vaccine potency, since the liver is thought to be a tolerogenic tissue.^{23–26} Despite these potential benefits, if miR-122 is present in antigen-presenting or other immune cells critical to generating an immune response, there could be a reduction in vaccine efficacy by including miRNA binding sites. To test whether

insertion location of miR-122 binding site in the 5' or 3' UTR of mRNA.

miR-122 binding sites reduce off-target liver expression after IM injection of LNP-mRNAs

Billions of LNP-mRNA SARS-CoV-2 vaccines were administered IM during the COVID-19 pandemic. While these were generally safe, there is potential for LNP-mRNA escape from the injection site to the liver, as evidenced in pre-clinical studies.^{8,9} Given this problem, we tested whether miR-122 de-targeting in LNP-mRNA could reduce off-target liver expression after IM injection. Mice were injected by the IM route, with LNPs encapsulating luciferase or miR-122 modified luciferase mRNA. Given that there was no significant difference between the number of copies or the location of insertion of miR-122 binding sites in the 5' or 3' UTR of the luciferase mRNA (Figures 1 and 2), we selected miR-122(2 \times)-luciferase as the representative modified mRNA for this experiment. IM injection of unmodified luciferase mRNA in LNPs mediated expression in the injected muscles, but it also mediated significant off-target luciferase expression in the livers of these animals (Figure 3A). By luciferase imaging, the amount of expression in the liver was approximately 2% of the signal observed in muscles that were injected with the unmodified luciferase mRNA-LNPs. In contrast, mice treated with miR-122(2 \times)-modified

integrating miR-122 binding sites preserves vaccine potency and perhaps improves it by avoiding antigen expression in the liver, we generated unmodified and miRNA binding-modified mRNA vaccines encoding EBOV VP40 matrix protein. Mice were immunized IM with LNPs carrying unmodified VP40 mRNA or VP40 mRNA modified with a single miR-122 binding sequence in the 5' or 3' UTR (LNP-miR122-VP40 and LNP-VP40-miR122, respectively). LNPs carrying luciferase mRNA (LNP-luciferase) were used as an irrelevant antigen control.

ELISAs were performed on sera collected 2, 6, and 12 weeks after single IM vaccination (Figure 4). No anti-VP40 immunoglobulin G (IgG) antibodies were detected in either untreated animals or control animals immunized with LNP-luciferase. In contrast, anti-VP40 IgG antibodies were detected in all VP40 mRNA vaccinated animals within 2 weeks of immunization. These antibodies peaked 6 weeks after these single immunizations, but they remained elevated through the end of the study at 12 weeks. Interestingly, the VP40 mRNA vaccine with a miR-122 binding site in its 5' UTR mediated higher VP40 antibody levels than the unmodified vaccine. Western blots of liver tissues after IM injection did not detect VP40 in miR-122-modified mRNA-treated mice (Figure S2A). However, when given larger doses IV, faint bands of VP40 were detected in the livers of mice treated

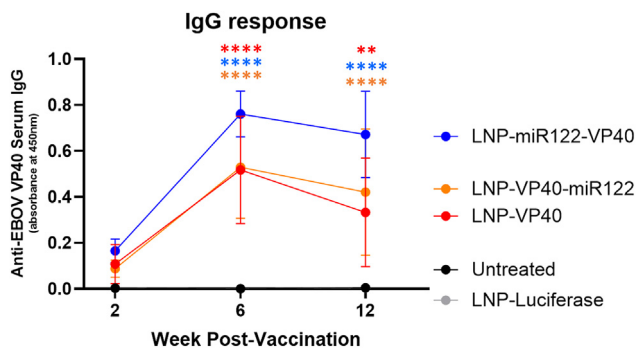


Figure 4. Antibodies produced after single vaccination with LNP-mRNA encoding EBOV VP40 with or without miR-122 binding site

Groups of six mice were vaccinated with 5 μ g LNP-mRNA in both quadriceps (10 μ g total) encoding either luciferase, EBOV VP40, or EBOV VP40 with a single miR-122 binding site. Sera were collected at weeks 2, 6, and 12 post-vaccination, and the presence of anti-EBOV VP40 IgG antibodies was quantified by ELISA. Statistics by two-way ANOVA; p values represent the difference between VP40 vaccinated animals and irrelevant antigen control mice (** $p \leq 0.01$; **** $p \leq 0.0001$). Data represents mean \pm SD.

with mRNA modified with the miR-122 binding site in the 3' UTR but not in mice treated with 5' UTR binding site insertions (Figure S2B). These data show that the addition of miR-122 binding sites does not have a negative impact on IgG response and may boost efficacy if antigen is more completely restricted in the liver.

DISCUSSION

This study reinforces the utility of miR-122 binding sites to mitigate off-target hepatic expression of LNP-mRNA therapeutics. We hypothesized that large doses to the liver via IV injection would reveal apparent weaknesses in liver de-targeting if any of the miR-122-modified mRNAs harbored less-effective combinations of miR-122 binding sites. LNP-mRNAs modified with miR-122 binding sites reduced luciferase expression in the liver by up to 99% (Figure 2) when given IV, showing the potency of these binding site sequences to restrict the expression of modified mRNAs. When mice received IM injections of unmodified luciferase mRNA, leakage from the injection site and off-target expression was clearly seen in the liver (Figure 3A). Consistent with our IV data, we were able to control this off-target expression in the liver by 95% (Figure 3D) with miR-122 binding site-modified LNP-mRNA.

Importantly, the inclusion of miR-122 binding sites did not diminish the mRNA expression in the injected muscle tissue. In fact, the luciferase activity in the injected muscle of miR(2 \times)-luciferase mice was slightly higher than those treated with unmodified luciferase (Figures 3A and 3C). In 293 cells in culture, there was a slight increase in expression by mRNAs with two miRNA targets when compared to mRNAs with 0, 1, or 5 of the 5' miRNA targets (Figure 1B), but these differences were not statistically significant. This suggests that perhaps the two copies of the miRNA targets serendipitously formed a more easily expressed mRNA, but again, this was not statistically

different. Another possible explanation is the increase in muscle luciferase activity was caused by an increase in luciferin substrate availability to the muscle due to a lack of liver expression of luciferase in the miR-122 binding site-modified mRNA group. With minimal luciferase expressed in the liver, circulating luciferin would not be depleted in the liver and would continue to circulate until reaching the muscle, where the majority of luciferase is expressed. This is also an important insight if using miRNA de-targeting for therapeutics delivering enzyme encoding mRNA, where efficacy could be gained in the target tissue by not having the necessary substrate depleted by off-target tissues.

As little as one copy of the miR-122 binding site was sufficient to significantly reduce LNP-mRNA expression in the liver. No further statistically significant decreases in liver signal were seen as more binding site sequences were added (Figures 1 and 2). This differs from others using miR-122 binding sites to de-target DNA-based adeno-associated virus (AAV) vectors showing greater transgene repression in the liver cells when more miR-122 binding sites were added.^{13,14,17} AAV vectors, which have a DNA genome, exhibit a gradual increase in transgene expression that stabilizes over the course of days to weeks.²⁷ The kinetics of AAV expression and other DNA viral vectors are opposites of LNP-mRNA vectors, which deliver a burst of mRNA, and expression degrades rapidly after delivery. With the sustained expression of viral DNA vectors, multiple miR-122 binding sites appear to provide added benefit. On the other hand, our data show that adding extra binding sites to mRNA payloads results in diminishing returns (Figures 1 and 2). This is consistent with Jain et al.,²⁰ where one and three binding sites performed similarly. Adding fewer binding site sequences while retaining liver de-targeting could reduce the problems associated with having multiple repetitive sequences in the IVT template DNA or mRNA, such as recombination of the IVT DNA template and the formation of undesirable secondary mRNA structures.

miR-122 binding site location in the 5' or 3' UTR also did not significantly alter the liver de-targeting effect (Figures 1 and 2). In our study, miR-122 binding sites were primarily inserted into the 5' UTRs, which differ from others in the field, predominately 3' insertions.^{16–18,20,21} Insertions in the 3' UTR logically follow mammalian endogenous mRNAs, which have miRNA binding sites mainly in the 3' UTR.²⁸ Our decision to insert our miR-122 binding sites primarily in the 5' UTR is supported by experiments conducted by Lytle et al. that show that repression of a gene was equally effective in DNA plasmids containing 5' or 3' UTR miRNA binding sites.²⁹

When used in an LNP-mRNA vaccine encoding EBOV VP40, inclusion of miR-122 binding sites did not negatively affect the anti-VP40 IgG antibody response (Figure 4). This is important because if miR-122 was present in cells critical to antigen presentation and antibody response, we could have seen reductions in IgG levels compared to unmodified mRNA. Anti-VP40 IgG levels in animals immunized with LNP-miR122-VP40 were even higher than those immunized with unmodified LNP-VP40 or LNP-VP40-miR122. This was

surprising, given that the loss of a fraction of expression that would otherwise be expressed in the liver might damage the immune response. Conversely, eliminating expression in the liver might have had the opposite effect since the liver is a site of immune tolerance induction.^{23–26} Therefore, avoiding antigen expression in the liver could boost mRNA vaccine potency by avoiding liver-mediated tolerance to the antigen. In fact, some groups have intentionally targeted the liver with LNP-mRNA encoding food, self, or environmental antigens to exploit its tolerogenic nature to treat food or environmental allergies as well as autoimmune antigens.^{30–32}

Avoiding antigen expression in the liver could be particularly advantageous for LNP-mRNA vaccines due to the need for repetitive booster doses as with COVID-19 mRNA vaccines, increasing opportunities for vector leakage into the bloodstream. Considering that mRNA vaccines generate cytotoxic T lymphocytes (CTLs) as a mechanism of their vaccine action, it may be prudent to de-target their expression from the liver since these CTLs may kill hepatocytes that are transfected when the vaccines are boosted. This may cause liver damage in proportion to the number of hepatocytes that are transfected. miRNA-122 expression de-targeting may therefore protect the liver and the patient from their own immune system.

We did not detect VP40 in livers receiving miRNA-modified mRNAs after IM injection. However, we did detect vaccine protein expression in the liver after IV injections of the miRNA-modified mRNAs, but only in the 3' modified LNP-VP40-miR122. We did not observe VP40 in the 5' miRNA-modified mRNA (Figure S2). This could partially explain the difference in IgG response seen between 5' and 3' modified mRNAs. This is somewhat contradictory to our reporter data showing that 5' vs. 3' insertions did not mediate a significant difference in liver de-targeting; however, tissues for western blot were taken 8 h after injection versus 18 h after in reporter studies. These data suggest that the different combinations of miR-122 binding sites performed equivalently for overall expression de-targeting of bulk doses of mRNA, but there may be differences in mRNA degradation kinetics at early time points.

Although this study provides insight into the efficacy of miRNA to de-target the liver, this approach has several limitations. First, miR-122 binding sites do not prevent LNP particles from distributing to and entering cells in the liver. Therefore, side effects due to mistargeting of the nanoparticle's lipid components themselves could still occur. Strategies to target LNPs to specific tissues at some level must avoid cholesterol binding to ApoE to prevent unintended targeting to hepatocytes. In addition, re-targeting efforts can include conjugation of active receptor binding moieties to particles³³ or manipulation of the particle charge.^{34,35} These targeting and de-targeting efforts can be combined with miRNA expression de-targeting to increase vaccine and therapeutic efficacy while minimizing off-target effects. Second, care must be taken to ensure that miR-122 is not expressed in the tissue that needs to be treated. This can be particularly challenging in diseased tissue, where miRNA expression varies from healthy tissue. Finally, our studies use mouse models to serve as a proof of concept.

However, the extent of leakage of LNP-mRNA vaccines to the liver in humans is unclear.

In conclusion, the data presented here show the utility of miR-122 binding sites to reduce off-target liver expression in LNP-mRNA therapeutics. Integrating miRNA de-targeting with other targeting strategies can maximize on-target effects while avoiding off-target side effects like immune tolerization and CTL killing of host cells during vaccine boosting.

MATERIALS AND METHODS

IVT mRNA plasmid construction

DNA plasmids were constructed as template IVT. A firefly luciferase or EBOV VP40 gene was cloned into a plasmid containing an upstream T7 promoter and downstream polyadenylation tract. Oligonucleotides containing the miR-122 binding site sequence (caaacacatgtgcactcca) and PacI or NotI restriction site overhangs were annealed. IVT plasmids were digested with PacI or NotI and then ligated with the annealed oligos for insertion into the 5' or 3' UTR, respectively. The assembled plasmids were then linearized with ApeI to remove the plasmid backbone from the T7 cassette.

IVT mRNA synthesis

IVT was performed using the New England Biolabs (NEB) HiScribe T7 High Yield RNA Synthesis Kit (E2040S). Co-translational capping was performed using Trilink CleanCap Reagent AG (N-7113). To minimize immune activation and enhance protein expression, mRNAs were synthesized using N¹-methylpseudouridine-5'-triphosphate (Trilink, N-1081). After IVT, a DNAase treatment was performed on the mRNA to remove the DNA template. Purification of the mRNA was performed using a column-based purification method (NEB Monarch RNA Cleanup Kit, T2050) and run on a 1% agarose gel in an RNA denaturing dye to verify quality.

LNP assembly

LNPs were formulated with DSPC (Avanti polar lipids 850365P), cholesterol (Sigma, C3045), D-Lin-MC3-DMA (MedChemExpress, HY-112251), and DMG-PEG2000 (Avanti polar lipids 880151P) at a molar ratio of 10:48:40:2, respectively. Lipid stocks are diluted in 100% ethanol. Particle assembly was performed using the NanoAssemblr Ignite (Precision Nanosystems) microfluidics device. The mRNAs were diluted in 100 mM citrate buffer at pH 4 prior to mixing with the lipid mix in ethanol. Assembled LNPs were then diluted 40× in PBS (Ca²⁺/Mg²⁺ free) before concentration via Amicon Ultra-15 Centrifugal Filter (Millipore Sigma, UFC901096). The LNPs were filtered with a 0.2-μm syringe filter (Pall 4602 Acrodisc) and were then characterized by dynamic light scattering using a Zetasizer Advance Ultra Red (Malvern Panalytical, ZSU3305) to determine size, particle concentration, and zeta potential. LNPs were of consistent size (size ~80 nm, polydispersity index: 0.05, zeta potential: −5 mV). The nucleic acid content of the LNPs was determined by Quant-it RiboGreen RNA assay kit with and without Triton X-100 for LNP lysis to quantify encapsulated mRNA (Invitrogen, R11490).

In vitro experiments

Human cell lines 293T, A549, and Huh7 were seeded on black wall 96-well plates at a density of 12,500 cells per well and incubated overnight at 37°C, 5% CO₂. Cells were transfected with 100 ng mRNA with each LNP-mRNA and incubated again at 37°C, 5% CO₂ for 18 h. Luciferase activity was measured using the Bright-Glo Luciferase assay system (Promega, E2610) and a multiwell plate reader. These experiments were repeated once.

In vivo experiments

AAD mice (The Jackson Laboratory, B6.Cg-*Imm*p2^{Tg(HLA-A/H2-D)2Enge/J} strain no.: 004191) were injected either via IV tail vein or IM injections to the right quadriceps for luciferase reporter experiments. Mice were injected with 14 µg mRNA for IV experiments. Mice receiving IM injections of luciferase received 7 µg mRNA. Luciferase imaging was performed on all mice 18 h post-injection using an IVIS Lumina S5 (PerkinElmer). All reporter experiments were repeated once. For EBOV VP40 vaccines, BALB/c mice were given IM injections of 5 µg mRNA in both quadriceps (10 µg total). Blood was collected via cheek bleed, and serum was isolated using BD Microtainer collection tubes. VP40 vaccinations were performed once. Animals were housed in the Mayo Clinic animal facility, and all experiments were approved by the Mayo Clinic Institutional Animal Care and Use Committee. All animal experiments followed the guidelines of the Animal Welfare Act, Public Health Service Animal Welfare Policy, and the NIH *Guide for the Care and Use of Laboratory Animals*.

ELISA

ELISA plates (MaxiSorp, Thermo Fisher Scientific) were coated overnight at 4°C with 100 ng/well of recombinant EBOV VP40 (IBT Bioservices) diluted in 100 µL PBS. Plates were washed twice with 200 µL 1× Tris-buffered saline with 0.1% Tween 20 (TBS-T) before blocking with 200 µL 5% skim milk in TBS-T overnight at 4°C. After washing twice with 200 µL TBS-T, sera from each animal were tested in triplicate at a 1:1,000 dilution in 5% skim milk in TBS-T and were incubated for 2 h at room temperature. Plates were washed 4 times in 200 µL TBS-T. Then, goat anti-mouse IgG horseradish peroxidase (HRP) conjugated secondary antibody (Invitrogen) was added at a 1:10,000 dilution in 5% skim milk and incubated for 2 h at room temperature. Plates were washed four times with TBS-T. Then, 50 µL 1-Step Ultra TMB-ELISA (Thermo Fisher Scientific) was added to each well and incubated for 25 min at room temperature. Then, 50 µL 2 M sulfuric acid was added to stop the reaction. Absorbance was read at 450 nm using a Synergy H1 microplate reader (BioTek). Statistical analysis was performed by two-way ANOVA.

Western blotting

EBOV VP40 mRNA expression was tested by western blotting (Figure S1). The 293T cells were transfected with LNP-mRNAs containing miR-122 binding sites-modified or unmodified VP40. Cells were harvested 16 h after transfection. Total protein concentration was determined by bicinchoninic acid assay. We loaded 10 µg total protein into a 12% Mini-PROTEAN TGX gel (BioRad, 4561046). To detect VP40 in tissues, 10 mg liver and 30 mg muscle were lysed in

1 mL radioimmunoprecipitation assay buffer and homogenized using a Tissue Lyser II (Qiagen) at 25 Hz for 30 s, repeated twice for liver samples, and at 25 Hz for 2 min, repeated twice for muscle samples. We loaded 20 µg total protein onto a 12% SDS-PAGE gel. Semi-dry transfer was performed to transfer protein from the gel to a polyvinylidene fluoride (PVDF) membrane. Anti-EBOV VP40 primary antibody (IBT Bioservices, 0201-017) was diluted 1:2,000 in 5% skim milk in TBS-T and incubated overnight at 4°C. After washing the membrane, goat anti-mouse IgG HRP conjugated secondary antibody (Invitrogen) was added at a 1:10,000 dilution in 5% skim milk and incubated for 1 h at room temperature. The PVDF membrane was then developed with SuperSignal West Pico Plus chemiluminescent substrate (Thermo Scientific, 34580). Imaging was performed using BioRad ChemiDoc imaging system. For tissue western blots, livers were harvested 8 h after injection and snap-frozen on dry ice and then stored at −80°C. We cut 10 mg of each liver from the frozen tissue and homogenized it using a bead homogenizer to extract protein. We ran 10 µL of each sample per lane.

Statistical analysis

All statistical analysis was performed using GraphPad Prism version 10.2.3.

DATA AND CODE AVAILABILITY

Reasonable requests for materials, reagents, and data can be made by contacting the corresponding author.

ACKNOWLEDGMENTS

We would like to thank Matthew L. Hillestad for supplying us with an IVT plasmid template for our cloning. We also thank Nick M.G. Hoopingarner for technical assistance. This work was supported by NIH/NIAID grant no. R01 AI134937 to M.A.B. B.J.P. was supported by appointment to Mayo Clinic Graduate School T32 PhD Training Program in Virology and Gene Therapy 5T32AI132165. The graphical abstract for this manuscript was created using BioRender (<https://BioRender.com>).

AUTHOR CONTRIBUTIONS

Conceptualization, B.J.P. and S.Y.; formal analysis, B.J.P.; investigation, B.J.P.; methodology, B.J.P.; visualization, B.J.P.; resources, S.Y.; funding acquisition, M.A.B.; supervision, M.A.B.; writing – original draft, B.J.P.; writing – review & editing, B.J.P., M.A.B., and S.Y.

DECLARATION OF INTERESTS

The authors declare no competing interests.

SUPPLEMENTAL INFORMATION

Supplemental information can be found online at <https://doi.org/10.1016/j.omtm.2024.101402>.

REFERENCES

- Akinc, A., Maier, M.A., Manoharan, M., Fitzgerald, K., Jayaraman, M., Barros, S., Ansell, S., Du, X., Hope, M.J., Madden, T.D., et al. (2019). The Onpattro story and the clinical translation of nanomedicines containing nucleic acid-based drugs. *Nat. Nanotechnol.* 14, 1084–1087. <https://doi.org/10.1038/s41565-019-0591-y>.
- Hou, X., Zaks, T., Langer, R., and Dong, Y. (2021). Lipid nanoparticles for mRNA delivery. *Nat. Rev. Mater.* 6, 1078–1094. <https://doi.org/10.1038/s41578-021-00358-0>.
- Chaudhary, N., Weissman, D., and Whitehead, K.A. (2021). mRNA vaccines for infectious diseases: principles, delivery and clinical translation. *Nat. Rev. Drug Discov.* 20, 817–838. <https://doi.org/10.1038/s41573-021-00283-5>.

4. Warne, N., Ruesch, M., Siwik, P., Mensah, P., Ludwig, J., Hripsak, M., Godavarti, R., Prigodich, A., and Dolsten, M. (2023). Delivering 3 billion doses of Comirnaty in 2021. *Nat. Biotechnol.* *41*, 183–188. <https://doi.org/10.1038/s41587-022-01643-1>.
5. Akinc, A., Querbes, W., De, S., Qin, J., Frank-Kamenetsky, M., Jayaprakash, K.N., Jayaraman, M., Rajeev, K.G., Cantley, W.L., Dorkin, J.R., et al. (2010). Targeted delivery of RNAi therapeutics with endogenous and exogenous ligand-based mechanisms. *Mol. Ther.* *18*, 1357–1364. <https://doi.org/10.1038/mt.2010.85>.
6. Cullis, P.R., Chonn, A., and Semple, S.C. (1998). Interactions of liposomes and lipid-based carrier systems with blood proteins: Relation to clearance behaviour in vivo. *Adv. Drug Deliv. Rev.* *32*, 3–17. [https://doi.org/10.1016/s0169-409x\(97\)00128-2](https://doi.org/10.1016/s0169-409x(97)00128-2).
7. Sebastiani, F., Yanez Arteta, M., Lerche, M., Porcar, L., Lang, C., Bragg, R.A., Elmore, C.S., Krishnamurthy, V.R., Russell, R.A., Darwish, T., et al. (2021). Apolipoprotein E Binding Drives Structural and Compositional Rearrangement of mRNA-Containing Lipid Nanoparticles. *ACS Nano* *15*, 6709–6722. <https://doi.org/10.1021/acsnano.0c10064>.
8. Agency, E.M. (2021). Comirnaty COVID-19 mRNA Vaccine Assessment Report.
9. Agency, E.M. (2021). COVID-19 Vaccine Moderna Assessment Report.
10. Wilson, R.C., and Doudna, J.A. (2013). Molecular mechanisms of RNA interference. *Annu. Rev. Biophys.* *42*, 217–239. <https://doi.org/10.1146/annurev-biophys-083012-130404>.
11. Ruiz, A.J., and Russell, S.J. (2015). MicroRNAs and oncolytic viruses. *Curr. Opin. Virol.* *13*, 40–48. <https://doi.org/10.1016/j.coviro.2015.03.007>.
12. Ruiz, A.J., Hadac, E.M., Nace, R.A., and Russell, S.J. (2016). MicroRNA-Detargeted Mengovirus for Oncolytic Virotherapy. *J. Virol.* *90*, 4078–4092. <https://doi.org/10.1128/JVI.02810-15>.
13. Qiao, C., Yuan, Z., Li, J., He, B., Zheng, H., Mayer, C., Li, J., and Xiao, X. (2011). Liver-specific microRNA-122 target sequences incorporated in AAV vectors efficiently inhibits transgene expression in the liver. *Gene Ther.* *18*, 403–410. <https://doi.org/10.1038/gt.2010.157>.
14. Xie, J., Xie, Q., Zhang, H., Ameres, S.L., Hung, J.H., Su, Q., He, R., Mu, X., Seher Ahmed, S., Park, S., et al. (2011). MicroRNA-regulated, systemically delivered rAAV9: a step closer to CNS-restricted transgene expression. *Mol. Ther.* *19*, 526–535. <https://doi.org/10.1038/mt.2010.279>.
15. Geisler, A., and Fechner, H. (2016). MicroRNA-regulated viral vectors for gene therapy. *World J. Exp. Med.* *6*, 37–54. <https://doi.org/10.5493/wjem.v6.i2.37>.
16. Hordeaux, J., Buza, E.L., Jeffrey, B., Song, C., Jahan, T., Yuan, Y., Zhu, Y., Bell, P., Li, M., Chichester, J.A., et al. (2020). MicroRNA-mediated inhibition of transgene expression reduces dorsal root ganglion toxicity by AAV vectors in primates. *Sci. Transl. Med.* *12*, eaba9188. <https://doi.org/10.1126/scitranslmed.aba9188>.
17. Geisler, A., Jungmann, A., Kurreck, J., Poller, W., Katus, H.A., Vetter, R., Fechner, H., and Müller, O.J. (2011). microRNA122-regulated transgene expression increases specificity of cardiac gene transfer upon intravenous delivery of AAV9 vectors. *Gene Ther.* *18*, 199–209. <https://doi.org/10.1038/gt.2010.141>.
18. Cawood, R., Chen, H.H., Carroll, F., Bazan-Peregrino, M., van Rooijen, N., and Seymour, L.W. (2009). Use of tissue-specific microRNA to control pathology of wild-type adenovirus without attenuation of its ability to kill cancer cells. *PLoS Pathog.* *5*, e1000440. <https://doi.org/10.1371/journal.ppat.1000440>.
19. Selvam, A.K., Jawad, R., Gramignoli, R., Achour, A., Salter, H., and Björnstedt, M. (2021). A Novel mRNA-Mediated and MicroRNA-Guided Approach to Specifically Eradicate Drug-Resistant Hepatocellular Carcinoma Cell Lines by Selenomethionine. *Antioxidants* *10*, 1094. <https://doi.org/10.3390/antiox10071094>.
20. Jain, R., Frederick, J.P., Huang, E.Y., Burke, K.E., Mauger, D.M., Andrianova, E.A., Farlow, S.J., Siddiqui, S., Pimentel, J., Cheung-Ong, K., et al. (2018). MicroRNAs Enable mRNA Therapeutics to Selectively Program Cancer Cells to Self-Destruct. *Nucleic Acid Ther.* *28*, 285–296. <https://doi.org/10.1089/nat.2018.0734>.
21. Hewitt, S.L., Bailey, D., Zielinski, J., Apte, A., Musenge, F., Karp, R., Burke, S., Garcon, F., Mishra, A., Gurumurthy, S., et al. (2020). Intratumoral IL12 mRNA Therapy Promotes TH1 Transformation of the Tumor Microenvironment. *Clin. Cancer Res.* *26*, 6284–6298. <https://doi.org/10.1158/1078-0432.CCR-20-0472>.
22. Roces, C.B., Lou, G., Jain, N., Abraham, S., Thomas, A., Halbert, G.W., and Perrie, Y. (2020). Manufacturing Considerations for the Development of Lipid Nanoparticles Using Microfluidics. *Pharmaceutics* *12*, 1095. <https://doi.org/10.3390/pharmaceutics12111095>.
23. Horst, A.K., Neumann, K., Diehl, L., and Tiegs, G. (2016). Modulation of liver tolerance by conventional and nonconventional antigen-presenting cells and regulatory immune cells. *Cell. Mol. Immunol.* *13*, 277–292. <https://doi.org/10.1038/cmi.2015.112>.
24. McMurphy, T.B., Park, A., Heizer, P.J., Bottenfield, C., Kurasawa, J.H., Ikeda, Y., and Doran, M.R. (2024). AAV-mediated co-expression of an immunogenic transgene plus PD-L1 enables sustained expression through immunological evasion. *Sci. Rep.* *14*, 28853. <https://doi.org/10.1038/s41598-024-75698-2>.
25. Ronca, V., Gerussi, A., Collins, P., Parente, A., Oo, Y.H., and Invernizzi, P. (2024). The liver as a central "hub" of the immune system: pathophysiological implications. *Physiol. Rev.* *19*, 1. <https://doi.org/10.1152/physrev.00004.2023>.
26. Liu, Y., Yang, H., Li, T., and Zhang, N. (2024). Immunotherapy in liver cancer: overcoming the tolerogenic liver microenvironment. *Front. Immunol.* *15*, 1460282. <https://doi.org/10.3389/fimmu.2024.1460282>.
27. Malik, A.K., Monahan, P.E., Allen, D.L., Chen, B.G., Samulski, R.J., and Kurachi, K. (2000). Kinetics of recombinant adeno-associated virus-mediated gene transfer. *J. Virol.* *74*, 3555–3565. <https://doi.org/10.1128/jvi.74.8.3555-3565.2000>.
28. Gu, S., Jin, L., Zhang, F., Sarnow, P., and Kay, M.A. (2009). Biological basis for restriction of microRNA targets to the 3' untranslated region in mammalian mRNAs. *Nat. Struct. Mol. Biol.* *16*, 144–150. <https://doi.org/10.1038/nsmb.1552>.
29. Lytle, J.R., Yario, T.A., and Steitz, J.A. (2007). Target mRNAs are repressed as efficiently by microRNA-binding sites in the 5' UTR as in the 3' UTR. *Proc. Natl. Acad. Sci. USA* *104*, 9667–9672. <https://doi.org/10.1073/pnas.0703820104>.
30. Xu, X., Wang, X., Liao, Y.P., Luo, L., Xia, T., and Nel, A.E. (2023). Use of a Liver-Targeting Immune-Tolerogenic mRNA Lipid Nanoparticle Platform to Treat Peanut-Induced Anaphylaxis by Single- and Multiple-Epitope Nucleotide Sequence Delivery. *ACS Nano* *17*, 4942–4957. <https://doi.org/10.1021/acsnano.2c12420>.
31. Liu, Q., Wang, X., Liu, X., Kumar, S., Gochman, G., Ji, Y., Liao, Y.P., Chang, C.H., Situ, W., Lu, J., et al. (2019). Use of Polymeric Nanoparticle Platform Targeting the Liver To Induce Treg-Mediated Antigen-Specific Immune Tolerance in a Pulmonary Allergen Sensitization Model. *ACS Nano* *13*, 4778–4794. <https://doi.org/10.1021/acsnano.9b01444>.
32. Violatto, M.B., Casarin, E., Talamini, L., Russo, L., Baldan, S., Tondello, C., Messmer, M., Hintermann, E., Rossi, A., Passoni, A., et al. (2019). Dexamethasone Conjugation to Biodegradable Avidin-Nucleic-Acid-Nano-Assemblies Promotes Selective Liver Targeting and Improves Therapeutic Efficacy in an Autoimmune Hepatitis Murine Model. *ACS Nano* *13*, 4410–4423. <https://doi.org/10.1021/acsnano.8b09655>.
33. Breda, L., Papp, T.E., Triebwasser, M.P., Yadegari, A., Fedorky, M.T., Tanaka, N., Abdulmalik, O., Pavani, G., Wang, Y., Grupp, S.A., et al. (2023). In vivo hematopoietic stem cell modification by mRNA delivery. *Science* *381*, 436–443. <https://doi.org/10.1126/science.ad6967>.
34. Cheng, Q., Wei, T., Farbiak, L., Johnson, L.T., Dilliard, S.A., and Siegwart, D.J. (2020). Selective organ targeting (SORT) nanoparticles for tissue-specific mRNA delivery and CRISPR-Cas gene editing. *Nat. Nanotechnol.* *15*, 313–320. <https://doi.org/10.1038/s41565-020-0669-6>.
35. Dilliard, S.A., Cheng, Q., and Siegwart, D.J. (2021). On the mechanism of tissue-specific mRNA delivery by selective organ targeting nanoparticles. *Proc. Natl. Acad. Sci. USA* *118*, e2109256118. <https://doi.org/10.1073/pnas.2109256118>.